

# Inverse Scattering Method Solves the Problem of Full Statistics of Nonstationary Heat Transfer in the Kipnis-Marchioro-Presutti Model

Eldad Bettelheim,<sup>1,\*</sup> Naftali R. Smith,<sup>2,3,†</sup> and Baruch Meerson<sup>1,‡</sup>

<sup>1</sup>*Racah Institute of Physics, Hebrew University of Jerusalem, Jerusalem 91904, Israel*

<sup>2</sup>*Laboratoire de Physique de l'École Normale Supérieure, CNRS,*

*ENS & Université PSL, Sorbonne Université, Université de Paris, 75005 Paris, France*

<sup>3</sup>*Department of Solar Energy and Environmental Physics, Blaustein Institutes for Desert Research, Ben-Gurion University of the Negev, Sede Boqer Campus, 8499000, Israel*

We determine the full statistics of nonstationary heat transfer in the Kipnis-Marchioro-Presutti lattice gas model at long times by uncovering and exploiting complete integrability of the underlying equations of the macroscopic fluctuation theory. These equations are closely related to the derivative nonlinear Schrödinger equation (DNLS), and we solve them by the Zakharov-Shabat inverse scattering method (ISM) adapted by Kaup and Newell (1978) for the DNLS. We obtain explicit results for the exact large deviation function of the transferred heat for an initially localized heat pulse, where we uncover a nontrivial symmetry relation.

*Introduction.* – The Kipnis-Marchioro-Presutti (KMP) model is a prototypical stochastic lattice gas model of heat transfer, for which the Fourier's law of heat diffusion at a coarse-grained level was proven rigorously [1]. The model consists of immobile particles occupying a whole lattice and carrying continuous amounts of energy. At each stochastic move the total energy of a randomly chosen pair of nearest neighbors is randomly redistributed among them according to uniform distribution. In the last two decades the KMP model has become a paradigmatic model in the studies of fluctuations, including large deviations, of heat transfer in classical many-body systems out of thermal equilibrium [2–14].

Here we consider the KMP model on an infinite one-dimensional lattice and suppose that only one particle has a nonzero energy at  $t = 0$ . Due to the energy exchange with the neighbors, the energy will start spreading throughout the system. At times much longer than the inverse rate of the elemental energy exchange between the two neighbors (equal to  $1/2$ ), and at distances much larger than the lattice constant (equal to 1), the mean coarse-grained temperature  $\bar{u}(x, t)$  in the KMP model is governed by the heat diffusion equation [1, 15]  $\partial_t \bar{u}(x, t) = \partial_x^2 \bar{u}(x, t)$ . The initial temperature profile is a delta-function,  $\bar{u}(x, t = 0) = W\delta(x)$ , and so the solution is

$$\bar{u}(x, t) = (W/\sqrt{4\pi t}) \exp(-x^2/4t). \quad (1)$$

However, in stochastic realizations of the KMP model the coarse-grained temperature will fluctuate around the expected profile  $\bar{u}(x, t)$ , see Fig. 1. To characterize fluctuations of this non-stationary heat transfer, we will consider the total amount of heat  $W_>$ , observed on the right half line  $x > 0$  at time  $t = T \gg 1$ . The expected value of this quantity is, of course,  $W/2$ , and we will be interested in the full time-dependent statistics of the *heat excess*,  $J = \int_0^\infty u(x, t = T) dx - W/2$ . Obviously,  $\mathcal{P}(J, T)$ , the probability distribution of  $J$  at time  $T$ , has a compact support  $|J| \leq W/2$ .

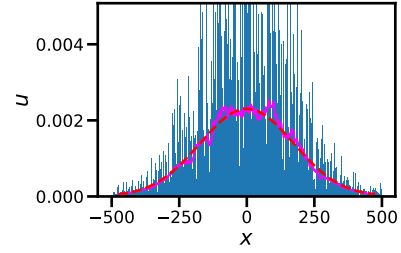


FIG. 1. Monte-Carlo simulation of the KMP model with  $W = 1$ . Plotted is the simulated temperature profile  $u$  as a function of  $x$  at time  $t = 3 \times 10^4$  (bars), its spatial average over each 50 consecutive lattice sites (solid line) and the theoretical Gaussian profile (1) (dashed line).

Similar non-stationary large-deviation settings, but with a *step-like* initial condition for the particle density or temperature, have been recently studied for a whole family of diffusive lattice gases [4, 7, 9, 16, 17], of which the KMP model is an important particular case. The main working tool in most of these studies has been the macroscopic fluctuation theory (MFT) [18], whose starting point is fluctuational hydrodynamics [15, 19]. For diffusive lattice gases with a single conservation law the fluctuational hydrodynamics has the form of a single macroscopic Langevin equation, which accounts for the fluctuational contribution to the flux of heat or mass. For the KMP model the Langevin equation reads

$$\partial_t u = \partial_x \left( \partial_x u + \sqrt{2}u\eta \right), \quad (2)$$

where  $u(x, t)$  is the temperature, and  $\eta(x, t)$  is a delta-correlated Gaussian noise:  $\langle \eta(x, t) \rangle = 0$  and  $\langle \eta(x, t)\eta(x', t') \rangle = \delta(x - x')\delta(t - t')$ .

At the core of the MFT [18] is a saddle-point evaluation of the path integral for the stochastic process, described by Eq. (2). The process starts from a specified initial condition and is conditioned on a large deviation in question.

The large deviation of our interest here is the heat excess defined above. The saddle-point evaluation of the path integral becomes accurate at long times,  $T \rightarrow \infty$ , due to the length scale separation between the heat diffusion length  $\sqrt{T}$  and the lattice constant. For the statistics of the heat (or mass) excess, the MFT equations and boundary conditions were derived in Ref. [4], and we will present them shortly. The solution of the MFT problem describes the *optimal path* of the process: the most likely time history of the temperature field  $u(x, t)$  which dominates the probability distribution  $\mathcal{P}(J, T)$  that we are after. The MFT problem, however, has proven to be very hard to solve analytically, especially for quenched (deterministic) initial conditions [20]. In particular, for the KMP model, only small- $J$  [7] and large- $J$  [9] asymptotics have been obtained until now (but for a step-like initial condition). This Letter reports a major advance in this area of statistical mechanics by presenting an exact solution to this problem by uncovering and exploiting complete integrability of the underlying MFT equations. We obtain explicit results for an initially localized heat pulse,  $u(x, t = 0) = W\delta(x)$ , by finding a nontrivial symmetry, specific to this initial condition.

*Formulation of the MFT problem.* – Let us recap the formulation of the MFT problem for the statistics of heat excess at time  $T$  [4]. First we re-scale the variables  $t$ ,  $x$  and  $u$  by  $T$ ,  $\sqrt{T}$  and  $W/\sqrt{T}$ , respectively. The optimal path is described by two coupled Hamilton's equations: partial differential equations for the re-scaled temperature field  $u(x, t)$  and the conjugate “momentum density” field  $p(x, t)$ . It is convenient to introduce the (minus) momentum density gradient field  $v(x, t) = -\partial_x p(x, t)$ . In the variables  $u$  and  $v$ , the MFT equations are [4, 9]

$$\partial_t u = \partial_x(\partial_x u + 2u^2 v), \quad (3)$$

$$\partial_t v = \partial_x(-\partial_x v + 2uv^2). \quad (4)$$

The re-scaled initial condition is

$$u(x, t = 0) = \delta(x). \quad (5)$$

The condition on the heat excess at  $t = T$  becomes

$$\int_0^\infty u(x, t = 1) dx - \frac{1}{2} = j \equiv \frac{J}{W}. \quad (6)$$

The minimization of the action functional, that enters the constrained path integral, with respect to variations of  $u(x, t)$  yields, aside from Eqs. (3) and (4), yields a second boundary condition in time [4],

$$v(x, t = 1) = -\lambda \delta(x), \quad (7)$$

where  $\lambda$  plays the role of a Lagrange multiplier, to be ultimately fixed by the constraint (6).

Once  $u(x, t)$  and  $v(x, t)$  are found, one can calculate the re-scaled mechanical action, which can be written as [4, 7, 9]

$$s = \int_0^1 dt \int_{-\infty}^\infty dx u^2 v^2. \quad (8)$$

The action yields the probability density  $\mathcal{P}(J, T, W)$  up to a pre-exponent:

$$\ln \mathcal{P}(J, T, W) \simeq -\sqrt{T} s \left( \frac{J}{W} \right). \quad (9)$$

A crucial and previously unappreciated observation is that Eqs. (3) and (4) coincide with the derivative nonlinear Shrödinger (DNLS) equation in imaginary time and space [21]. The DNLS equation (with real time and space) describes propagation of nonlinear electromagnetic waves in plasmas and other media [22]. An initial-value problem for the DNLS equation is completely integrable via the Zakharov-Shabat inverse scattering method (ISM) adapted by Kaup and Newell for the DNLS [22]. The heat excess problem presents an additional difficulty, as here one needs to solve a boundary-value problem in time, rather than an initial-value problem. Here we overcome this difficulty by (i) exploiting a previously unknown symmetry relation [23], specific to the initial condition (5):

$$v(x, t) = -\lambda u(-x, 1 - t), \quad (10)$$

and (ii) making use of a shortcut that allows one to determine the rate function  $s(j)$  even without the knowledge of  $u(x, t)$  and  $v(x, t)$  for all  $t$ .

*Solution of the MFT problem.*– Equations (3) and (4) belongs to a class of integrable systems for which a Lax pair exists, *i.e.*, they are equivalent to the compatibility condition of a system of two linear differential equations. The latter system defines scattering amplitudes which depend on  $u$  and  $v$ . The idea behind the approach that we shall use – the ISM – is to consider the time evolution of these scattering amplitudes, which turns out to be very simple, as shown below. By relating these scattering amplitudes, at  $t = 0$  and  $t = 1$ , to the fields  $u$  and  $v$ , the method will enable us, while exploiting the symmetry (10), to find the heat excess  $j = j(\lambda)$  which suffices for the calculation of  $s = s(j)$ .

Adapting the derivation of Kaup and Newell [22] to imaginary time and space, we consider the linear system

$$\begin{cases} \partial_x \boldsymbol{\psi}(x, t, k) = U(x, t, k) \boldsymbol{\psi}(x, t, k), \\ \partial_t \boldsymbol{\psi}(x, t, k) = V(x, t, k) \boldsymbol{\psi}(x, t, k), \end{cases} \quad (11)$$

where  $\boldsymbol{\psi}(x, t, k)$  is a column vector of dimension 2,

$$U(x, t, k) = \begin{pmatrix} -ik/2 & -iv\sqrt{ik} \\ -iu\sqrt{ik} & ik/2 \end{pmatrix}, \quad V(x, t, k) = \begin{pmatrix} k^2/2 - ikuv & -i(\sqrt{ik})^3 v + i\sqrt{ik}v_x - i\sqrt{ik}2v^2u \\ -i(\sqrt{ik})^3 u + i\sqrt{ik}u_x - i\sqrt{ik}2u^2v & -k^2/2 + ikuv, \end{pmatrix}, \quad (12)$$

and  $k$  is a spectral parameter. As one can check, the compatibility condition  $\partial_t \partial_x \psi = \partial_x \partial_t \psi$ , which corresponds to

$$\partial_t U - \partial_x V + [U, V] = 0, \quad (13)$$

is indeed equivalent to Eqs. (3) and (4).

Let us define the matrix  $\mathcal{T}(x, y, t, k)$  as the  $x$ -propagator of the system (11), namely, the solution to

$$\partial_x \mathcal{T}(x, y, t, k) = U(x, t, k) \mathcal{T}(x, y, t, k) \quad (14)$$

with  $\mathcal{T}(x, x, t, k) = I$  (the identity matrix). At  $x \rightarrow \pm\infty$ , where the fields  $u(x, t)$  and  $v(x, t)$  vanish, the matrix  $U$  becomes very simple,

$$U(x \rightarrow \pm\infty, t, k) = \begin{pmatrix} -ik/2 & 0 \\ 0 & ik/2 \end{pmatrix}. \quad (15)$$

Therefore, it is natural to define the full-space propagator  $T(t, k)$  as follows:

$$T(t, k) = \lim_{\substack{x \rightarrow \infty \\ y \rightarrow -\infty}} \begin{pmatrix} e^{ikx/2} & 0 \\ 0 & e^{-ikx/2} \end{pmatrix} \times \mathcal{T}(x, y, t, k) \begin{pmatrix} e^{-iky/2} & 0 \\ 0 & e^{iky/2} \end{pmatrix}. \quad (16)$$

The entries of the matrix  $T(t, k)$  are precisely the scattering amplitudes of the system (11). The time evolution of  $T(t, k)$  is easy to find. Indeed, the matrix  $\mathcal{T}(x, y, t, k)$  satisfies:

$$\partial_t \mathcal{T}(x, y, t, k) = V(x, t, k) \mathcal{T}(x, y, t, k) - \mathcal{T}(x, y, t, k) V(y, t, k). \quad (17)$$

One can check that Eq. (17) is compatible with (14) (*i.e.*  $\partial_t \partial_x T = \partial_x \partial_t T$ ) due to Eq. (13). The matrix  $V(x, t, k)$  too becomes very simple in the limit  $x \rightarrow \pm\infty$ ,

$$V(x \rightarrow \pm\infty, t, k) = \frac{k^2}{2} \begin{pmatrix} 1 & 0 \\ 0 & -1 \end{pmatrix}. \quad (18)$$

Plugging (18) into (17), one finds the time evolution of  $\mathcal{T}(x \rightarrow \infty, y \rightarrow -\infty, t, k)$  which in turn, using (16), yields that of  $T(t, k)$ :

$$T(t, k) = \begin{pmatrix} a(t, k) & \tilde{b}(t, k) \\ b(t, k) & \tilde{a}(t, k) \end{pmatrix} = \begin{pmatrix} a(0, k) & \tilde{b}(0, k)e^{k^2 t} \\ b(0, k)e^{-k^2 t} & \tilde{a}(0, k) \end{pmatrix} \quad (19)$$

where we have introduced here a notation for the matrix elements of  $T(t, k)$ .

Plugging the temporal boundary conditions (5) and (7), we calculate  $T(0, k)$  and  $T(1, k)$  explicitly by solving Eq. (14), see [24]. Comparing the two solutions and using (19) we obtain

$$ik [Q_+(k) + Q_-(k)] - ikQ_-(k) \times ikQ_+(k) = -\lambda i k e^{-k^2} \quad (20)$$

where  $Q_{\pm}(k)$  are the Fourier transforms of  $v(z, 0)$  restricted to the positive and negative real axes, respectively

$$Q_-(k) = \int_{-\infty}^0 v(z, 0) e^{ikz} dz, \quad Q_+(k) = \int_0^{\infty} v(z, 0) e^{ikz} dz. \quad (21)$$

We solve Eq. (20) in [24], with the result

$$ikQ_{\pm}(k) = 1 - (1 \pm v_{\pm}) e^{\Phi_{\pm}(k)}, \quad (22)$$

$$\Phi_{\pm}(k) = \pm \int_{-\infty}^{\infty} \frac{\ln(1 + i\lambda k' e^{-k'^2})}{k' - k \mp i0^+} \frac{dk'}{2\pi i}, \quad (23)$$

where  $v_{\pm} = v(0^{\pm}, 0)$ .

To compute  $v_{\pm}$ , we demand that  $Q_{\pm}(k)$  be regular at the origin, corresponding to a vanishing  $v(z, 0)$  at infinity. Setting  $k = 0$  in Eq. (22) and using the Sokhotski-Plemelj formula

$$\int_{-\infty}^{\infty} \frac{f(k)}{k \pm i0^+} \frac{dk}{2\pi i} = \int_{-\infty}^{\infty} \frac{f(k)}{k} \frac{dk}{2\pi i} \mp \frac{1}{2} f(0), \quad (24)$$

we obtain after some algebra

$$\pm v_{\pm} = \exp \left[ \mp \int_{-\infty}^{\infty} \arctan(\lambda k' e^{-k'^2}) \frac{dk'}{2\pi k'} \right] - 1. \quad (25)$$

Taking the derivative of Eq. (22) with respect to  $k$  at  $k = 0$ , yields [24]

$$Q_+(0) = \frac{1}{4\pi} \int_{-\infty}^{\infty} \frac{\ln(1 + \lambda^2 k^2 e^{-2k^2})}{k^2} dk - \frac{\lambda}{2}. \quad (26)$$

Figure 2 shows  $\text{Re } Q_+(k)$  and  $\text{Im } Q_+(k)$  versus  $k$  at  $\lambda = 1$ , obtained by plugging Eq. (25) for  $v_{\pm}$  into Eq. (22). This figure also shows the same quantities computed by solving Eqs. (3) and (4) numerically with a back-and-forth iteration algorithm [25]. The analytical and numerical curves are almost indistinguishable.

Using Eqs. (6), (10) and (21) alongside with the conservation law  $\int_{-\infty}^{\infty} u(x, t) dx = 1$ , we determine  $j = j(\lambda)$ :

$$j(\lambda) = \frac{Q_+(0)}{\lambda} + \frac{1}{2} = \frac{1}{4\pi\lambda} \int_{-\infty}^{\infty} \frac{\ln(1 + \lambda^2 k^2 e^{-2k^2})}{k^2} dk. \quad (27)$$

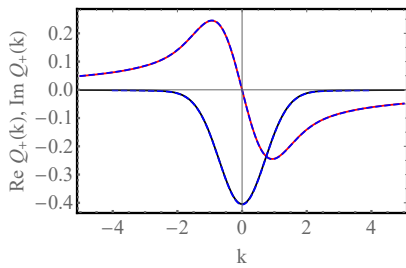


FIG. 2. Analytical results for  $Q_+(k)$ , described by Eqs. (22), (23) and (25) (solid lines), versus numerical results (dashed lines) for  $\lambda = 1$ , or  $j = 0.09568\dots$ . The symmetric and anti-symmetric curves show  $\text{Re } Q_+(k)$  and  $\text{Im } Q_+(k)$ , respectively.

Now we use an additional shortcut, which makes the results we have obtained so far sufficient for obtaining the rate function  $s = s(j)$ . The shortcut comes in the form of the relation  $ds/dj = \lambda$ , which is a consequence of the fact that  $j$  and  $\lambda$  are conjugate variables, see *e.g.* Ref. [26]. It allows one to calculate  $s(j)$  bypassing Eq. (8) [which would require the knowledge of the whole optimal path  $u(x, t)$ ]. We have

$$\frac{ds}{d\lambda} = \frac{ds}{dj} \frac{dj}{d\lambda} = \lambda \frac{dj}{d\lambda} = \frac{dQ_+(0)}{d\lambda} - \frac{Q_+(0)}{\lambda}. \quad (28)$$

Using Eq. (26), we integrate Eq. (28) with respect to  $\lambda$  to get

$$s(\lambda) = Q_+(0) + \int_{-\infty}^{\infty} \frac{\text{Li}_2\left(-\lambda^2 k^2 e^{-2k^2}\right)}{8\pi k^2} dk + \frac{\lambda}{2}. \quad (29)$$

where  $\text{Li}_2(z) = \sum_{k=1}^{\infty} z^k/k^2$  is the dilogarithm function,  $Q_+(0)$  is given by Eq. (26), and the integration constant was determined from  $s(\lambda = 0) = 0$ . Equations (27) and (29) give the complete rate function  $s(j)$  in a parametric form and represent the main results of this work.

Figure 3 shows  $s(j)$  alongside with two asymptotics:  $j \rightarrow 0$  and  $|j| \rightarrow 1/2$ , which correspond to  $\lambda \rightarrow 0$  and  $|\lambda| \rightarrow \infty$ , respectively. The asymptotic  $\lambda \rightarrow 0$  can be obtained either from the exact rate function (27) and (29) [24], or from a perturbative expansion applied directly to the MFT equations [7]. Here, by virtue of the symmetry (10), it can be obtained very easily. Indeed, in the leading order in  $\lambda \ll 1$ , Eq. (8) gives

$$s(\lambda) \simeq \lambda^2 \int_0^1 dt \int_{-\infty}^{\infty} dx \bar{u}^2(x, t) \bar{u}^2(-x, 1-t) = \frac{\lambda^2}{8\sqrt{2\pi}}, \quad (30)$$

where we used the zeroth-order, mean-field solution (1), rescaled by  $W$ . The shortcut relation  $ds/dj = \lambda$  can be rewritten as  $(ds/d\lambda)(d\lambda/dj) = \lambda$ . Combined with Eq. (30) it yields  $s(j \rightarrow 0) \simeq \sqrt{8\pi}j^2$ .

The asymptotic of  $|\lambda| \rightarrow \infty$  is more subtle [24]. The

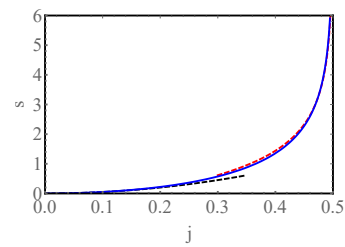


FIG. 3. The exact rate function  $Q_+(k)$ , given by Eqs. (27) and (29) (solid line) and two asymptotics:  $s(|j| \ll 1) = \sqrt{8\pi}j^2$  and Eq. (31) (dashed lines).

final result, already in terms of  $j$ , is

$$s(|j| \rightarrow 1/2) \simeq \frac{4 \left[ -\frac{1}{2} W_{-1} \left( -\frac{1}{2} \pi^2 \Delta^2 \right) \right]^{3/2}}{3\pi} = \frac{4}{3\pi} \ln^{3/2} \left( \frac{2}{\pi \Delta} \sqrt{\ln \frac{2}{\pi \Delta}} \sqrt{\ln \frac{2}{\pi \Delta}} \dots \right), \quad (31)$$

where  $\Delta \equiv 1/2 - |j| \ll 1$ , and  $W_{-1}(\dots)$  is the proper branch of the product log (Lambert  $W$ ) function [27].

*Discussion.*— By combining the MFT and the ISM, we calculated exactly the rate function  $s(j)$ , see Eqs. (27) and (29), which describes the full statistics of nonstationary heat transfer in the KMP model at long times. We achieved this goal for an initially localized heat pulse, where a simplification comes from the nontrivial symmetry relation (10). The optimal history of the temperature profile  $u(x, t)$  proved difficult to obtain analytically, but it can be computed numerically [24]. A future work should address other initial conditions where non-stationary heat transfer statistics problems were previously solved analytically only in some limiting cases [4, 7, 9].

From a more general perspective, the optimal fluctuation method (OFM, a generic name which includes the MFT of lattice gases as a particular case) is a highly efficient tool which captures a broad class of large deviations of macroscopic systems. However, for non-stationary processes the OFM equations – coupled nonlinear partial differential equations for the optimal path – are usually very hard to solve exactly. One class of problems of this type has received a special attention: complete one-point height statistics of an interface, whose dynamics is described by the Kardar-Parisi-Zhang equation [28]. In this case the OFM captures the complete height statistics at short times [29–32]. Here too, a previous analytical progress in the solution of the OFM equations was limited to asymptotics of very large or very small interface height. But very recently these OFM equations have been solved exactly [33, 34] by exploiting exact integrability of the OFM equations for the KPZ problem, pointed out in Ref. [32]. Notably, the OFM equations of that problem coincide with the Nonlinear Schrödinger

equation, making the ISM, used in Refs. [33, 34], very suitable.

The research of E.B. and B.M. is supported by the Israel Science Foundation (grants No. 1466/15 and 1499/20, respectively). N.R.S. acknowledges support from the Yad Hanadiv fund (Rothschild fellowship).

---

\* eldad.bettelheim@mail.huji.ac.il

† naftalismsmith@gmail.com

‡ meerson@mail.huji.ac.il

- [1] C. Kipnis, C. Marchioro and E. Presutti, J. Stat. Phys. **27**, 65 (1982).
- [2] L. Bertini, A. De Sole, D. Gabrielli, G. Jona-Lasinio, and C. Landim, Phys. Rev. Lett. **94**, 030601 (2005).
- [3] T. Bodineau and B. Derrida, Phys. Rev. E **72**, 066110 (2005).
- [4] B. Derrida and A. Gerschenfeld, J. Stat. Phys. **137**, 978 (2009).
- [5] V. Lecomte, A. Imparato, and F. van Wijland, Prog. Theor. Phys. Suppl. **184**, 276 (2010).
- [6] P. I. Hurtado and P. L. Garrido, Phys. Rev. Lett. **107**, 180601 (2011).
- [7] P. L. Krapivsky and B. Meerson, Phys. Rev. E **86**, 031106 (2012).
- [8] A. Prados, A. Lasanta, and P. I. Hurtado, Phys. Rev. E **86**, 031134 (2012).
- [9] B. Meerson and P. V. Sasorov, J. Stat. Mech. (2013) P12011.
- [10] M. A. Peletier, F. H. J. Redig, and K. Vafayi, J. Math. Phys. **55**, 093301 (2014).
- [11] L. Zarfaty and B. Meerson, J. Stat. Mech. (2016) 033304.
- [12] O. Shpielberg, Y. Don, and E. Akkermans, Phys Rev E **95**, 032137 (2017).
- [13] C. Gutiérrez-Ariza and P. I. Hurtado, J. Stat. Mech. (2019) 103203.
- [14] R. Frassek, C. Giardinà, and J. Kurchan, SciPost Phys. **9**, 054 (2020).
- [15] H. Spohn, *Large Scale Dynamics of Interacting Particles* (Springer, New York, 1991)
- [16] B. Meerson and P. V. Sasorov, Phys. Rev. E **89**, 010101 (Rapid Communication) (2014).
- [17] A. Vilenkin, B. Meerson and P. V. Sasorov, J. Stat. Mech. (2014) P06007.
- [18] L. Bertini, A. De Sole, D. Gabrielli, G. Jona-Lasinio, and C. Landim, Rev. Mod. Phys. **87**, 593 (2015).
- [19] C. Kipnis and C. Landim, *Scaling Limits of Interacting Particle Systems* (Springer, New York, 1999).
- [20] For an annealed step-like initial condition (a step-function with equilibrium density distributions with given average densities  $u_-$  and  $u_+$  at  $x < 0$  and  $x > 0$ ), the KMP problem was solved exactly by Derrida and Gerschenfeld [4]. They achieved it by uncovering an exact mapping between the KMP problem of the heat excess and the problem of density excess for the simple symmetric exclusion process, where an exact microscopic solution was previously obtained [35].
- [21] A standard form of the DNLS equation is

$$i\partial_t\phi + \partial_x^2\phi - i\partial_x(|\phi|^2\phi) = 0, \quad (32)$$

for a complex function  $\phi(x, t)$  [22]. The MFT equa-

tions (3) and (4) coincide with the equations for the real and imaginary parts of  $\phi(x, t)$ , following from Eq. (32), but in imaginary time and space.

- [22] D.J. Kaup and A.C. Newell. J. Math. Phys. **19**, 798 (1978).
- [23] Indeed, the symmetry relation (10) leaves Eqs. (3) and (4) and the boundary conditions (5) and (7) invariant.
- [24] See Supplemental Material at ...
- [25] A. I. Chernykh and M. G. Stepanov, Phys. Rev. E **64**, 026306 (2001).
- [26] F. D. Cunden, P. Facchi, and P. Vivo, J. Phys. A: Math. Theor. **49**, 135202 (2016).
- [27] <https://mathworld.wolfram.com/LambertW-Function.html>.
- [28] M. Kardar, G. Parisi, and Y.-C. Zhang, Phys. Rev. Lett. **56**, 889 (1986).
- [29] I. V. Kolokolov and S. E. Korshunov, Phys. Rev. B **75**, 140201(R) (2007); Phys. Rev. B **78**, 024206 (2008); Phys. Rev. E **80**, 031107 (2009).
- [30] B. Meerson, E. Katzav, and A. Vilenkin, Phys. Rev. Lett. **116**, 070601 (2016).
- [31] A. Kamenev, B. Meerson, and P. V. Sasorov, Phys. Rev. E **94**, 032108 (2016).
- [32] M. Janas, A. Kamenev, and B. Meerson, Phys. Rev. E **94**, 032133 (2016).
- [33] A. Krajenbrink and P. Le Doussal, Phys. Rev. Lett. **127**, 064101 (2021).
- [34] A. Krajenbrink and P. Le Doussal, arXiv:2107.13497.
- [35] B. Derrida and A. Gerschenfeld, J. Stat. Phys. **136**, 1 (2009).

Supplementary Material for

“Inverse Scattering Method Solves the Problem of Full Statistics of Nonstationary Heat Transfer in the Kipnis-Marchioro-Presutti Model” by E. Bettelheim *et al.*

Here we give some technical details of the calculations described in the main text of the Letter.

**I. SOLVING THE SCATTERING PROBLEM AT  $t = 0$  AND  $t = 1$**

Let us find the matrix  $\mathcal{T}(x, y, 0, k)$  at  $t = 0$ . By solving Eq. (14) of the main text at  $t = 0$ , using  $u(x, 0) = \delta(x)$ , one gets

$$\mathcal{T}(x, y, 0, k) = \begin{cases} \begin{pmatrix} e^{-ik(x-y)/2} & -i\sqrt{ik}/2 e^{-ik(x-y)/2} I_v(x, y) \\ 0 & e^{ik(x-y)/2} \end{pmatrix}, & xy > 0, \\ \begin{pmatrix} e^{ik(y-x)/2} [1 \pm ik I_v(x, 0)] & -i\sqrt{ik} e^{ik(y-x)/2} [I_u(x, y) \pm ik I_u(0, y) I_u(x, 0)] \\ \pm i\sqrt{ik} e^{ik(x+y)/2} & e^{ik(x-y)/2} \pm ik e^{ik(x+y)/2} I_u(0, y) \end{pmatrix}, & xy < 0, \end{cases} \quad (\text{S1})$$

where

$$I_v(x, y) = \int_y^x v(z) e^{ik(z-y)} dz, \quad I_u(x, y) = \int_y^x u(z, 1) e^{-ik(z-y)} dz, \quad (\text{S2})$$

and in the second case in (S1), the sign  $\pm$  is to be taken as the sign of  $y$ . Plugging (S1) into Eq. (16) of the main text, we compute  $T(0, k)$ :

$$T(0, k) = \begin{pmatrix} 1 - ikQ_+(k) & -i\sqrt{ik} [Q(k) - ikQ_-(k)Q_+(k)] \\ -i\sqrt{ik} & 1 - ikQ_-(k) \end{pmatrix} \quad (\text{S3})$$

in terms of  $Q_{\pm}(k)$  which are defined in Eq. (21) in the main text, with  $Q(k) = Q_+(k) + Q_-(k)$ .

It is useful to compare this result to the one obtained at  $t = 1$ . Here we have  $v(x, 1) = -\lambda\delta(x)$ . Similarly to the  $t = 0$  case, one gets

$$\mathcal{T}(x, y, 1, k) = \begin{cases} \begin{pmatrix} e^{-ik(x-y)/2} & 0 \\ -i\sqrt{ik} e^{ik(x-y)k/2} I_u(x, y) & e^{ik(x-y)/2} \end{pmatrix}, & xy > 0, \\ \begin{pmatrix} e^{-ik(x-y)/2} \pm \lambda ik e^{ik(x+y)/2} I_u(0, y) & \pm i\lambda\sqrt{ik} e^{-ik(x+y)/2} \\ -i\sqrt{ik} e^{ik(x-y)/2} [I_u(x, y) \pm \lambda ik I_u(0, y) I_u(x, 0)] & e^{ik(x-y)/2} [1 \pm \lambda ik I_u(x, 0)] \end{pmatrix}, & xy < 0, \end{cases} \quad (\text{S4})$$

where in the second case, the sign  $\pm$  is to be taken as the opposite of the sign of  $y$ . Now compute  $T(1, k)$ :

$$T(1, k) = \begin{pmatrix} 1 + \lambda ik R_+(k) & +i\lambda\sqrt{ik} \\ -i\sqrt{ik} [R(k) + \lambda ik R_-(k) R_+(k)] & 1 + \lambda ik R_-(k) \end{pmatrix} \quad (\text{S5})$$

where

$$R_+(k) = \int_{-\infty}^0 u(z, 1) e^{-ikz} dz, \quad R_-(k) = \int_0^{\infty} u(z, 1) e^{-ikz} dz, \quad R(k) = R_+(k) + R_-(k). \quad (\text{S6})$$

Comparing the upper-right elements of  $T(0, k)$  from Eq. (S3) and of  $T(1, k)$  from Eq. (S5), using Eq. (19) of the main text, leads to Eq. (20) of the main text.

## II. SOLVING EQ. (20) OF THE MAIN TEXT

We can complete the squares in Eq. (20) of the main text by writing

$$ikQ_{\pm}(k) = 1 - (1 \pm v_{\pm})e^{M_{\pm}(k)}, \quad (\text{S7})$$

where  $v_{\pm} = v(0^{\pm}, 0)$ . This turns Eq. (20) of the main text into

$$(1 + v_+) (1 - v_-) e^{M_+(k)+M_-(k)} = 1 + i\lambda k e^{-k^2}, \quad (\text{S8})$$

which has the solution

$$M_{\pm}(k) = \pm \int_{-\infty}^{\infty} \frac{\ln(1 + i\lambda k' e^{-k'^2})}{k' - k \mp i0^+} \frac{dk'}{2\pi i} \quad (\text{S9})$$

provided the condition

$$(1 + v_+) (1 - v_-) = 1 \quad (\text{S10})$$

is satisfied. Eq. (S9) is derived by noting that  $Q_{\pm}$  are analytic in the upper and lower half plane respectively and are well-behaved when  $k$  is allowed to reach infinity through the respective half-planes. We then use the well-known decomposition  $f(k) = f_+(k) + f_-(k)$  of a general function  $f(k)$  into functions analytic in the upper and lower half-planes,  $f_{\pm}(k)$ , respectively, given by  $f_{\pm}(k) = \int \frac{f(k')}{k' - k \mp i0^+} \frac{dk'}{2\pi i}$ . This decomposition is applied to the logarithm of Eq. (S8). Plugging Eq. (S9) into Eq. (S7), we obtain the solution given in Eqs. (22) and (23) of the main text.

## III. CALCULATING $Q_+(0)$

Taking the derivative of Eq. (22) with respect to  $k$  at  $k = 0$ , yields the equation:

$$\begin{aligned} Q_+(0) &= i(1 + v_+) \frac{d}{dk} \exp \left[ \int_{-\infty}^{\infty} \frac{\ln(1 + i\lambda k' e^{-k'^2})}{k' - k} \frac{dk'}{2\pi i} + \frac{1}{2} \ln(1 + i\lambda k e^{-k^2}) \right]_{k=0} \\ &= i \frac{d}{dk} \left[ \int_{-\infty}^{\infty} \frac{\ln(1 + i\lambda k' e^{-k'^2})}{k' - k} \frac{dk'}{2\pi i} + \frac{1}{2} \ln(1 + i\lambda k e^{-k^2}) \right]_{k=0} = \\ &= \int_{-\infty}^{\infty} \frac{\ln(1 + i\lambda k' e^{-k'^2})}{k'^2} \frac{dk'}{2\pi} - \frac{\lambda}{2} \end{aligned} \quad (\text{S11})$$

The imaginary part of the integrand is an odd function of  $k$  and therefore does not contribute to the integral. Keeping only the real part and simplifying it, we obtain (26) of the main text, where we replaced the principal value integral by a regular integral since the integrand is regular at  $k = 0$ .

## IV. ASYMPTOTICS OF SMALL AND LARGE $\lambda$

At small  $\lambda$  Eq. (26) of the main text yields

$$Q_+(0)(\lambda \ll 1) \simeq \frac{1}{4\pi} \int_{-\infty}^{\infty} \frac{\lambda^2 k^2 e^{-2k^2}}{k^2} dk - \frac{\lambda}{2} = -\frac{\lambda}{2} + \frac{\lambda^2}{4\sqrt{2\pi}}, \quad (\text{S12})$$

therefore  $j(\lambda \ll 1) \simeq \lambda/(4\sqrt{2\pi})$ . Now, using the  $|z| \ll 1$  asymptotic  $\text{Li}_2(-z) \simeq -z$  in the integrand of Eq. (29), we obtain after a simple algebra:  $s(\lambda \ll 1) \simeq \lambda^2/(8\sqrt{2\pi})$ . This yields the asymptotic behavior  $s(j \ll 1) \simeq 2\sqrt{2\pi} j^2$  given in the main text.

Now we consider the  $|\lambda| \gg 1$  asymptotic and start from Eq. (26). For simplicity we consider only  $\lambda > 0$  due to the symmetry  $j(-\lambda) = -j(\lambda)$ ,  $s(-\lambda) = s(\lambda)$ . It is convenient to calculate the asymptotic of the derivative  $dQ_+(0)/d\lambda$ . Denote the integrand in Eq. (26) by

$$F(\lambda, k) = \frac{\ln\left(1 + \lambda^2 k^2 e^{-2k^2}\right)}{k^2}.$$

Then taking the derivative of (26) of the main text with respect to  $\lambda$ , we find

$$\frac{dQ_+(0)}{d\lambda} = \frac{1}{4\pi} \int_{-\infty}^{\infty} \frac{\partial F(\lambda, k)}{\partial \lambda} dk - \frac{1}{2}, \quad \frac{\partial F}{\partial \lambda} = \frac{2\lambda}{\lambda^2 k^2 + e^{2k^2}}. \quad (\text{S13})$$

For  $\lambda \gg 1$  the integral over  $k$  is dominated by the region  $|k|\lambda \lesssim 1$  where we can replace  $e^{2k^2}$  by 1. An important subleading contribution comes from a region around  $|k| \sim \sqrt{\ln \lambda}$ . To proceed, we write down the exact relation

$$\frac{\partial F}{\partial \lambda} = \frac{2\lambda}{\lambda^2 k^2 + 1} + \delta(\lambda, k), \quad (\text{S14})$$

where

$$\delta(\lambda, k) = \frac{2\lambda}{\lambda^2 k^2 + e^{2k^2}} - \frac{2\lambda}{\lambda^2 k^2 + 1}. \quad (\text{S15})$$

Integrating the first term in Eq. (S14) with respect to  $k$  from  $-\infty$  to  $\infty$ , we obtain the leading contribution to the integral in (S13) at  $\lambda \gg 1$ , which is equal to  $1/2$ , cancelling out with the last term in (S13).  $\delta(\lambda, k)$  is very small at  $k \lesssim \sqrt{\ln \lambda}$ , it reaches a minimum at  $k \simeq \sqrt{\ln \lambda}$ , and it is dominated by the second term in Eq. (S15) at  $k \gtrsim \sqrt{\ln \lambda}$ . To obtain the subleading contribution to  $dQ_+(0)/d\lambda$  with a logarithmic accuracy, we can evaluate the integral over  $|k|$  from a cutoff at  $|k| = \sqrt{\ln \lambda}$  to  $\infty$ , i.e., we approximate

$$\delta(\lambda, k) \simeq -\frac{2\lambda}{\lambda^2 k^2 + 1} \theta\left(|k| - \sqrt{\ln |\lambda|}\right), \quad (\text{S16})$$

a good approximation except for a narrow boundary layer around  $|k| = \sqrt{\ln \lambda}$ , see Fig. 4. Using the approximation

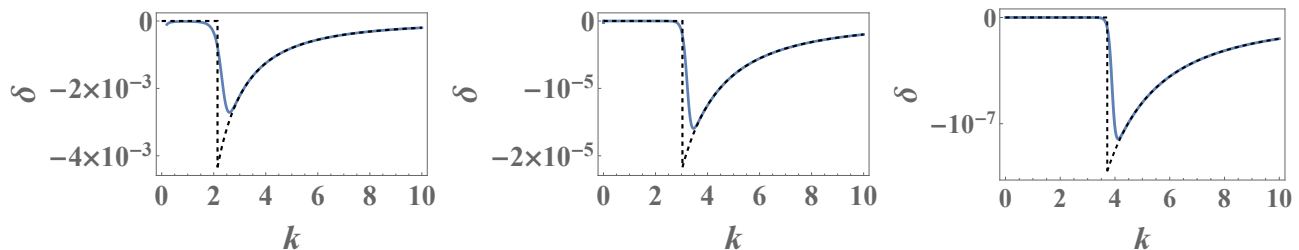


FIG. 4. The exact  $\delta(\lambda, k)$  given by (S15) (solid line) and the approximation (S16) (dashed line), for different values of  $\lambda$ : (a)  $10^2$ , (b)  $10^4$  and (c)  $10^6$ . The approximation can be seen to slowly (logarithmically) improve as  $\lambda$  is increased.

(S16) in (S13), we find

$$\frac{dQ_+(0)}{d\lambda} \simeq -\frac{1}{\pi \lambda \sqrt{\ln \lambda}}. \quad (\text{S17})$$

Integrating (S17) with respect to  $\lambda$  we obtain (footnote: the integration constant is unimportant in the limit  $\lambda \gg 1$  that we consider here as it only gives a subleading correction)

$$Q_+(0) \simeq -\frac{2\sqrt{\ln \lambda}}{\pi}. \quad (\text{S18})$$

As a result, using the connection (27) between  $j$  and  $Q_+(0)$ ,

$$j(\lambda \gg 1) \simeq \frac{1}{2} - \frac{2\sqrt{\ln \lambda}}{\pi \lambda}. \quad (\text{S19})$$



To calculate the large- $\lambda$  asymptotic of  $s(\lambda)$ , we plug (S19) into the first equality in (28) to get

$$\frac{ds}{d\lambda} = \lambda \frac{dj}{d\lambda} \simeq \frac{2\sqrt{\ln \lambda}}{\pi\lambda} \quad (\text{S20})$$

Integrating this over  $\lambda$  we obtain (footnote: the integration constant is unimportant in the limit  $\lambda \gg 1$  that we consider here)

$$s(\lambda \gg 1) \simeq \frac{4}{3\pi} (\ln \lambda)^{3/2}. \quad (\text{S21})$$

Solving Eq. (S19) for  $\lambda$ , we obtain

$$\lambda \left( j \rightarrow \left( \frac{1}{2} \right)^- \right) \simeq e^{-\frac{1}{2} W_{-1}(-\frac{1}{2} \pi^2 \Delta^2)}, \quad (\text{S22})$$

where  $\Delta \equiv 1/2 - j \ll 1$ , and  $W_{-1}(\dots)$  is the proper branch of the product log (Lambert  $W$ ) function [27]. Plugging Eq. (S22) into Eq. (S21), we obtain the large- $j$  asymptotic (31) of the main text.

## V. OBTAINING THE OPTIMAL PATH $u(x, t)$ NUMERICALLY AT ALL TIMES

Our exact solution gives the rate function  $s(j)$  but it does not give the optimal path  $u(x, t)$  at all times. To calculate the latter analytically, one would need to solve Eq. (14) of the main text at arbitrary times  $0 \leq t \leq 1$ , and this is far more challenging than solving it only at  $t = 0$  and  $t = 1$ , as we did. The optimal path can, however, be computed numerically, using the back-and-forth iteration algorithm due to Chernykh and Stepanov [25]. The results of one such calculation are shown in Fig. 5.

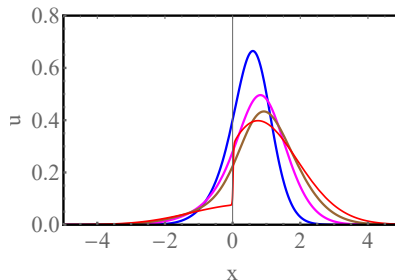


FIG. 5. The optimal temperature profile  $u(x, t)$  for  $\lambda = 10$  (corresponding to  $j \simeq 0.38$ ) at times  $1/4$ ,  $1/2$ ,  $3/4$  and  $1$ . Noticeable is a shock-like singularity of  $u$  at  $x = 0$  and  $t = 1$ .